

## A new story of cyclodextrin as a bulky pendent group causing uncommon behaviour to random copolymers in solution†

Fuji Sakai, Guosong Chen\* and Ming Jiang\*

Received 27th December 2011, Accepted 19th January 2012

DOI: 10.1039/c2py00614f

A series of random copolymers poly[(*N*-isopropyl acrylamide)-*co*-(aminoethyl methacrylate  $\beta$ -cyclodextrin)] (PNiCD) were synthesized by free radical polymerization, followed by examination of their physical properties to measure  $\langle R_g \rangle$ ,  $\langle R_h \rangle$ ,  $M_w$  and  $A_2$  using dynamic and static light scattering (DLS and SLS). The cyclodextrin (CD) moiety attached to the main chain plays two roles. As supramolecular host moieties, CDs form inclusion complexes with guest-ended polymers, leading to “graft-like” copolymers. As bulky hydrophilic moieties, CDs stabilize the micelles induced by the “coil-to-globule” transition of NIPAM segments as temperature increases. The studies of heating rate dependency of this self-assembly of PNiCD are performed by a combination of DLS, SLS, AFM and TEM. Based on tracing the evolution of the size distributions of the aggregates of PNiCD at different heating rates and AFM observations, two mechanisms for the aggregation have been proposed as follows: in slow heating, the copolymer chains form unimolecular micelles first and then second aggregation of the micelles takes place leading to a large but loose aggregates; in fast heating, random aggregation occurs directly leading to small and compact aggregates. The formation of the unimolecular micelles as building blocks for the following aggregation, which was observed exclusively in slow heating process, was not reported before for PNIPAM and the corresponding copolymers. This can be attributed to the presence of the pendent bulky CD groups making the copolymer chains rigid, which has been addressed.

### Introduction

Micellization of block copolymers has been one of the hottest research areas in chemistry and materials science for more than thirty years.<sup>1–4</sup> Plenty of morphologies and mechanisms of the micelles from a variety of block copolymers have been demonstrated.<sup>5–9</sup> Thanks to the toolbox provided by organic chemistry, in recent years more and more functional groups including supramolecular hosts or guests have been successively introduced into copolymers,<sup>10–20</sup> which has greatly extended the research field and made copolymers active in supramolecular chemistry and thus created a variety of new functional assemblies. In contrast to the wealth of insights for the huge family of block copolymers, the self-assembly mechanism of random copolymers still remains unclear, regardless some random copolymers have been reported to assemble into micellar structures<sup>21,22</sup> with

potential applications.<sup>21</sup> An obvious limitation of the related studies on random copolymers is the disordered monomer sequence preventing the chains from assembling into well-ordered morphologies, such as layered structure with a solvophobic core and a solvophilic shell as that in block copolymers. However, due to its simple preparation and practical applications, amphiphilic random copolymers are preferable and deep studies on mechanism and control of their self-assemblies are of great significance. In this paper, we focus on self-assembly of double hydrophilic random copolymer P[(*N*-isopropyl acrylamide)-*co*-(aminoethyl methacrylate  $\beta$ -cyclodextrin)] (PNiCD) consisting of temperature sensitive NIPAM units and hydrophilic pendent  $\beta$ -cyclodextrin groups. The design of this random copolymer is based on the following facts and considerations: the main part of the copolymer, *i.e.* the PNIPAM segments are temperature sensitive so that thermal induced self-assembly is possible; the side CD species is a bulky group which endows the random copolymer with some characters of a graft copolymer so the copolymer may show some peculiar characters in assembly and finally, the cavities of CD are available for constructing complex supramolecular graft copolymers *via* inclusion complexation *etc.* for further studies.

PNIPAM is one of the most well studied polymers showing the hydrophilic to hydrophobic transition at elevated temperature,

State Key Laboratory of Molecular Engineering of Polymers and Department of Macromolecular Science, Fudan University, 220 Handan Rd., Shanghai, 200433, China. E-mail: mjiang@fudan.edu.cn; guosong@fudan.edu.cn; Fax: +86 21 65643919; Tel: +86 21 65643919

† Electronic supplementary information (ESI) available: Zimm plot and <sup>1</sup>H-NMR of PNiCD copolymers, NMR and MALDI-TOF characterization of MPEG-ADA and MPEG-Azo, DLS results of cooling process. See DOI: 10.1039/c2py00614f

which brings the copolymer PNiCD temperature-triggered micellization behaviour. Based on the well-established mechanism of the coil-to-globule transition for single chain of PNIPAM, thermo-induced self-assembly of PNIPAM and its copolymer with some hydrophilic units has been extensively studied by experimental observations<sup>23–26</sup> and theoretical simulations.<sup>27–29</sup> Among this research, the kinetics and the dependence of the assembly on the heating rate have attracted much attention. All these are quite useful for us to understand the peculiar assembly behaviour of our copolymer PNiCD with bulky pendent CD groups.

Cyclodextrins (CDs) belong to a group of popular supramolecular hosts,<sup>30–33</sup> study of which started even earlier than that of the self-assembly of block copolymers. CD can accommodate various guest molecules inside its cavity. CD has a molecular weight comparable to an oligomer, *e.g.* 1135 for  $\beta$ -CD, but exists with a rigid shape and a diameter around 1 nm, thus it is expected that copolymers with pendant CDs differ in their self-assembly from those bearing other short hydrophilic branches, *e.g.* polyethylene glycol (PEG), poly(4-vinylpyridine) (P4VP) *etc.* Although linear homopolymers and copolymers containing CDs have been reported,<sup>18,34–39</sup> their micellization behaviour, especially that driven by external stimulus, has been rarely reported.<sup>17</sup> The present work focuses on self-assembly behaviour of random copolymer (PNiCD) consisting of NIPAM and  $\beta$ -CD containing monomer, which is simple and easy to prepare. The CD cavities as hosts on this copolymer are available for post-polymerization modifications by PEG with a guest end *via* inclusion complexation,<sup>17,19,34,36,40</sup> which can be tuned by the reversible nature of the host–guest pair. The heat-triggered aggregation behaviour of PNiCD was investigated using dynamic and static light scattering measurements (DLS and SLS) mainly with variation of three parameters, *i.e.* solution concentration, CD content, and heating rate. The obvious heating rate dependence of the size and distribution of the aggregates observed in PNiCD are very different from those reported before for PNIPAM and their copolymers. The new mechanism for the aggregation has been proposed for our new CD-containing copolymers.

## Experimental

### Materials

*N*-isopropylacrylamide (NIPAM) monomer was purchased from Tokyo Kasei Kogyo Co. and recrystallized three times from benzene/hexane (65 : 35 v/v) prior to use.  $\beta$ -CD was supplied by Sinopharm Chemical Reagent Co., and mono methoxy PEG ( $M_w = 2000$ ) (MPEG2k) was purchased from Alfar Aesar Co. Aminoethyl methacrylate CD (AEMACD) monomer was synthesized according to our reported procedure.<sup>17</sup> Unless otherwise mentioned, all other chemicals were used directly as received.

### Copolymerization of NIPAM and AEMACD

The desired amount (total weight of 300 mg) of AEMACD and NIPAM was dissolved in 3 mL deionized water. Then 3 mg of sodium persulfate and 1.5 mg of potassium sulfite were added and the solution was kept at 25 °C for 24 h under nitrogen after three freeze–thaw cycles. Then the solution was diluted with

water and dialyzed using a dialysis bag (MWCO 3500) for one week. Finally the product (PNiCD) was recovered by freeze-drying. Three samples namely PNiCD0.5, PNiCD1-1 and PNiCD1-2 were obtained using different feed ratios of the two monomers. PNIPAM homopolymer as a control sample was also prepared by this procedure.

### Synthesis of mono-end functionalized PEGs

The mono-end adamantane-functionalized polyethylene glycol (MPEG-ADA) was synthesized by reacting MPEG2k with 1-adamantane carbonyl chloride (1.2 equiv.) in dichloromethane (DCM) at room temperature for 24 h under nitrogen.<sup>17</sup> The resultant solution was precipitated in excess amount of diethyl ether and the precipitant was purified by silica column using chloroform/methanol as eluent (v:v = 10 : 1). The obtained sample was dried in a vacuum oven over night and characterized by NMR and MALDI-TOF mass spectrometry. For the preparation of mono-end azobenzene-functionalized PEG (MPEG-Azo), MPEG2k was first treated with succinyl anhydride (1.2 equiv.) and 2,4-dimethyl-3-aminopyridine (0.1 equiv.) in DCM under nitrogen at room temperature for 24 h to obtain mono-end carboxyl functionalized PEG (MPEG-COOH). Purified MPEG-COOH was then reacted with *p*-phenyl-azophenol (1.2 equiv.) in DCM under nitrogen at room temperature for 24 h by conventional esterification mediated by *N,N'*-dicyclohexylcarbodiimide (DCC). The purification and characterization method of MPEG-COOH and MPEG-Azo was the same as that of MPEG-ADA. Characterization details of these modified PEGs are shown in the ESI.†

### Characterization

SLS and DLS were performed to characterize the solution parameters of solvated copolymer chains as well as their aggregates using an ALV/5000E laser light scattering spectrometer, and the results are listed in Table 1. The Zimm plots of  $Kc/R$  against  $(q^2 + kc)$  of SLS for polymer solutions are shown in Fig. 1, where  $K = 4\pi n^2 (dn/dc)^2 / (N_A \lambda_0^4)$  is an optical constant, and  $q = (4\pi n / \lambda_0) \sin(\theta/2)$  in which  $N_A$ ,  $dn/dc$ ,  $n$ , and  $\lambda_0$  are Avogadro's number, specific refractive index increment, solvent refractive index, and wavelength of the light in a vacuum, respectively.  $R$  is the angular dependent excess absolute time-averaged scattered intensity.  $c$  is polymer concentration ( $\text{g mL}^{-1}$ ), and  $k$  is an arbitrary constant. The radius of gyration  $\langle R_g \rangle$ , second Virial coefficient  $A_2$ , and weight average molecular weight ( $M_w$ ) of polymers at 25 °C were obtained from the plot. The approximate  $M_w$  of the copolymer ( $c = 1.0 \text{ mg mL}^{-1}$ ) aggregates at elevated temperatures were estimated from the intercept of the linear plots of the Zimm plot. The refractive index increment  $dn/dc = 0.168 \text{ mL}^{-1}$  for the copolymer solution was determined by a differential refractometer, while that of the mixture of the copolymer and modified PEG,  $dn/dc = 0.151$ , was calculated from the weight averaged value of the neat PNiCD and PEG ( $dn/dc = 0.133$ ). For DLS measurements, CONTIN analysis was used for the measured autocorrelation curves to obtain the distribution of diffusion coefficients at a scattering angle of 90 °C in the temperature range of 25–50 °C. For the temperature scanning experiment to trace the self-assembly

**Table 1** Characterization of PNiCDs.  $M_w$ , and monomer unit ratio were determined by SLS and NMR, respectively. The average number of CDs on one chain was then calculated

Sample	Feed ratio (weight) (NIPAM : AEMACD)	$M_w/10^5 \text{ g mol}^{-1}$	Unit ratio (mol/mol) (NIPAM : AEMACD)	Average number of CDs on a chain
PNiCD0.5	1 : 0.5	3.62	49.3 : 1	60.9
PNiCD1-1	1 : 1	4.44	23.0 : 1	134
PNiCD1-2	1 : 1	1.22	24.1 : 1	39.2
PNIPAM	1 : 0	3.14	1 : 0	0

behaviour, the heating rates were chosen as 0.2, 0.33, 0.5, 1 °C min<sup>-1</sup>, stepwise heating at 1 °C for every 30 min (0.033 °C min<sup>-1</sup>), and direct heating by putting the sample cell into 50 °C water bath (approximate rate 30 °C min<sup>-1</sup>). Transmission electron microscopy (TEM) was performed on a Philips CM 120 electron microscope at accelerating voltage of 80 kV. A small drop of the sample solution at a desired temperature measurement was performed on Nanoscope IV Digital Instrument equipped with a silicon cantilever and E-type vertical engage piezoelectric scanner. The sample preparation was similar to that of TEM, but freshly cleaved mica was used as the substrate.

## Result and discussion

### Polymerization and characterization

Three PNiCD copolymers were synthesized by free radical copolymerization of NIPAM and AEMACD monomer. Their  $M_w$  and CD content were characterized by SLS and NMR, respectively. The average number of CDs on each chain was also calculated from the ratio of the integrated area of the characteristic peaks belong to NIPAM and CD. A control sample of neat PNIPAM was also prepared using the same method (Table 1). Synthesis of MPEG-ADA and MPEG-Azo was confirmed by NMR and MALDI-TOF MS, and their  $M_n$  was determined to be 2.1 k and 2.2 k, respectively.

### Solution behaviour of PNiCDs in water and non-covalent grafting of guest polymers

We studied the aqueous solutions PNiCD at 25 °C by SLS and DLS first. The Zimm plots of PNiCD1-2 are shown in Fig. 1

(other data are shown in Fig. S1†). Three parameters were estimated, *i.e.* weight-average molecular weight ( $M_w$ ), radius of gyration ( $\langle R_g \rangle$ ), and second Virial coefficients ( $A_2$ ), which are summarized in Table 2 together with hydrodynamic radius ( $\langle R_h \rangle$ ) obtained from DLS. From the data, two characteristic features for the dissolved state of PNiCD1-2 are noteworthy. One is the ratio of  $\langle R_g \rangle / \langle R_h \rangle$ , reaching 2.05. Generally,  $\langle R_g \rangle / \langle R_h \rangle$  reflects the conformation of polymer chains, *i.e.* for flexible chains in good solvent,  $\langle R_g \rangle / \langle R_h \rangle$  lies in the range of 1.5–1.8, while for extended chains, it is close to or larger than 2.0. Compared to the value 1.46 measured for homopolymer PNIPAM with typical random coil conformation, the significantly larger  $\langle R_g \rangle / \langle R_h \rangle$  of PNiCD1-2 reflects its extended chain conformation, as a result of the steric hindrance of the densely attached pendent bulky CDs. Another characteristic feature is the negative value of  $A_2$  ( $-7.3 \times 10^{-7} \text{ mol L g}^{-2}$ ) for PNiCD1-2 while that for PNIPAM is nearly zero. It means that water is not a good solvent for PNiCD1-2 as a result of hydrogen bonding existing between CDs although they are hydrophilic.

Mixing MPEG-ADA with PNiCD1-2 in solution caused substantial changes in  $\langle R_g \rangle$ , from 29.1 to 42.8 nm and  $\langle R_h \rangle$  from 14.2 nm to 20.2 nm, as shown in Fig. 1 and Table 2. Meanwhile, the intensity of the scattered light also showed a significant increase. These results demonstrate the formation of a large molecular species, *i.e.* supramolecular graft copolymer PNiCD-PEG-1, composed of PNiCD main chain and MPEG-ADA grafts due to the inclusion complexation between the CD side groups in the former and the end ADA group in the latter. However, the  $\langle R_g \rangle / \langle R_h \rangle$  value changes a little, indicating that the grafting of PEG-ADA to PNiCD does not alter the extended conformation of the main chain. Note that the measured  $M_w$  of PNiCD-PEG-1 ( $1.30 \times 10^5$ ), which is only slightly larger than

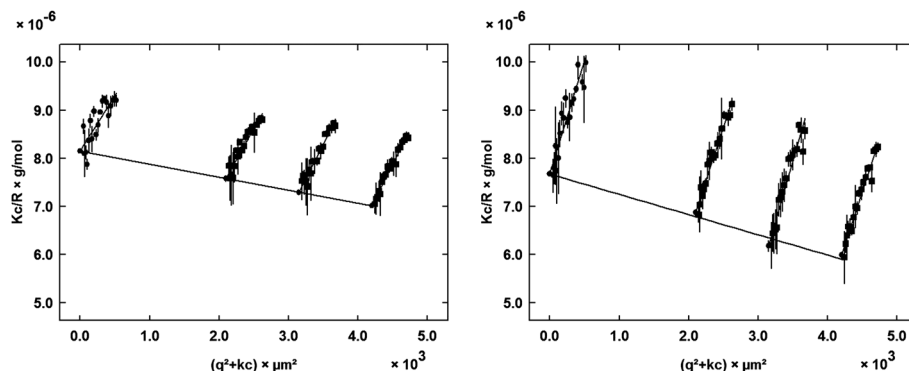


**Fig. 1** Zimm plots of neat PNiCD1-2 (left) and complex PNiCD-PEG-1 (right) in water. The concentrations of neat PNiCD1-2 solutions are 0.4, 0.6, and 0.8 mg mL<sup>-1</sup>. In PNiCD-PEG-1, one equiv. of MPEG-ADA was mixed with PNiCD1-2.

**Table 2**  $\langle R_h \rangle$ ,  $\langle R_g \rangle$ ,  $M_w$ ,  $A_2$ , and scattered light intensity of PNiCD1-2, PNiCD-PEG-1, PNiCD-PEG- $\alpha$ CD, PNiCD-PEG- $\beta$ CD, and PNIPAM for control. The corresponding volume ratios of each sample to neat copolymer calculated from  $\langle R_h \rangle$  are shown in brackets

	PNIPAM	PNiCD1-2	PNiCD-PEG-1	PNiCD-PEG- $\alpha$ CD	PNiCD-PEG- $\beta$ CD
$\langle R_h \rangle$ /nm	22.3	14.2	20.2 (2.86)	23.5 (4.50)	14.6 (1.08)
$\langle R_g \rangle$ /nm	32.6	29.1	42.8	—	—
$\langle R_g \rangle / \langle R_h \rangle$	1.46	2.05	2.12	—	—
$M_w / 10^5$ g mol <sup>-1</sup>	3.14	1.22	1.30 <sup>a</sup>	—	—
$A_2 / 10^{-7}$ mol L g <sup>-2</sup>	0.0	-7.3	-6.2 <sup>a</sup>	—	—
Intensity	—	20.1	35.5	46.7	24.3

<sup>a</sup> The datum is not accurate because of the concentration dependency of inclusion complexation.

that of PNiCD itself, is underestimated because the *real* concentration of the graft copolymer in solution is lower than the given value as a result of only partial grafting of the PEG-ADA chains.

As the complex of PNiCD-PEG-1 is a supramolecular graft copolymer, just like “supramolecular block copolymer” that have been extensively studied recently,<sup>36,41–43</sup> the structures, architectures and even further dissociation can be realized by supramolecular means. As shown in Table 2, when five equivalents of  $\alpha$ -CDs were added to the solution of the complex PNiCD-PEG-1, both  $\langle R_h \rangle$  and scattered light intensity increased, *i.e.* from 20.2 nm to 23.4 nm, and 35.5 to 46.7, respectively (namely PNiCD-PEG- $\alpha$ CD). Considering the strong ability of  $\alpha$ -CD to be threaded by the PEG chain as well as its weak binding ability with ADA compared to that of  $\beta$ -CD, it is reasonable to attribute the substantial increase of  $\langle R_h \rangle$  and intensity to the formation of grafts of polypseudorotaxane (PPR) composed of the PEG chains and threaded  $\alpha$ -CDs (Fig. 2). Furthermore, when  $\beta$ -CD was further added into the solution of PNiCD-PEG- $\alpha$ CD (namely PNiCD-PEG- $\beta$ CD), a drastic decrease of  $\langle R_h \rangle$ , from 23.5 nm to 14.6 nm was observed, very close to that of PNiCD (14.2 nm) alone. Obviously the large amount of added free  $\beta$ -CD could compete with the bonded  $\beta$ -CD in PNiCD capturing the PEG-ADA chains from the supramolecular graft copolymer leading to its dissociation.

Azo species have a peculiar feature as a guest molecule from its photoresponsive *trans*–*cis* isomerization. Since its *trans*-isomer forms much stronger inclusion complex with  $\beta$ -CD than its *cis*-isomer, the complex shows photo-responsive association/dissociation under the irradiation of UV or visible light. After

MPEG-Azo was added,  $\langle R_h \rangle$  of PNiCD1-1 increased (Table 3), showing that a complex was formed by PNiCD1-1 and MPEG-Azo (PNiCD-PEG-2). The size increase here is not as significant as that of PNiCD-PEG-1, probably because the binding ability of azo with  $\beta$ -CD is weaker than that of ADA.<sup>32</sup> However, this supramolecular graft copolymer shows interesting photo-responsive properties. After UV light ( $\lambda = 365$  nm) irradiation for 10 min,  $\langle R_h \rangle$  of the solution dropped to the original value of PNiCD indicating the dissociation of the complex. The change in the scattered light intensity demonstrated the same process.

### Self-assembly behaviour of copolymer PNiCD

As a random copolymer composed of PNIPAM segments mainly and pendent bulky CDs, PNiCD is expected to show thermally induced self-assembly because both the main chain of PNiCD and side groups of CD are hydrophilic at room temperature but PNiCD would turn amphiphilic when the temperature is increased to above the LCST (lower critical solution temperature) of PNIPAM chains. Thus PNiCD would form aggregates with a micelle-like structure in which hydrophilic CD groups enrich the surface. In this work, thermally induced aggregation of PNiCD1-1 in water was investigated by DLS and SLS with emphasis on its dependence on heating rates (Table 4).  $\langle R_h \rangle$  changes of PNiCD1-1 in aqueous solution (1.0 mg mL<sup>-1</sup>) with increasing temperature from 25 °C to 48 °C at six different heating rates, from 0.003 °C min<sup>-1</sup> to 30 °C min<sup>-1</sup> were monitored (Table 4). A common feature of the five curves in Fig. 3a is that at low temperature,  $\langle R_h \rangle$  is rather small (about 25 nm) and changes a little below 35 °C, and then suddenly increases at about 37 °C, showing onset of aggregation, and finally reaches a plateau of much higher  $\langle R_h \rangle$  values at around 45 °C. However, the more important fact is that, the heating rate clearly affected the aggregation behaviour and the size of the resultant aggregates, *i.e.* slow heating rate resulted in larger sizes while fast rate led to smaller sizes. As shown in Table 4, the final  $\langle R_h \rangle$  reached 45 nm and 130 nm for the quickest (30 °C min<sup>-1</sup>) and the slowest (0.033 °C min<sup>-1</sup>) heating, respectively.

**Table 3**  $\langle R_h \rangle$  and scattered light intensity of PNiCD1-1 and its complex PNiCD-PEG-2 before and after UV irradiation. The corresponding volume ratio to neat copolymer calculated from  $\langle R_h \rangle$  is in brackets

	PNiCD1-1/nm	PNiCD-PEG-2/nm	PNiCD-PEG-2 (UV)/nm
$\langle R_h \rangle$	24.7	27.3 (1.48)	24.2 (0.94)
Intensity	28.2	29.1	27.9

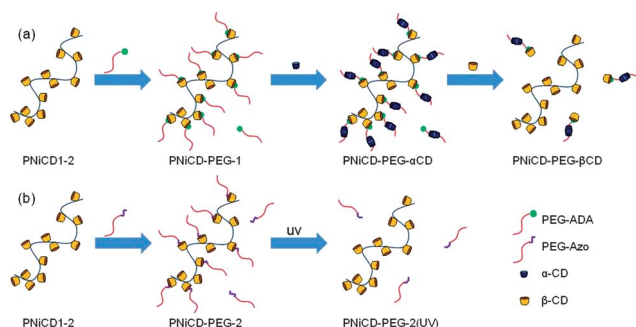


**Fig. 2** Schemes of the inclusion complexation process: (a) formation of PNiCD-PEG-1, followed by subsequent addition of  $\alpha$ -CD (PNiCD-PEG- $\alpha$ CD) and then competitive  $\beta$ -CD (PNiCD-PEG- $\beta$ CD). (b) The complexation between PNiCD and MPEG-Azo (PNiCD-PEG-2) followed by UV irradiation.

**Table 4**  $\langle R_h \rangle$ , PDI,  $M_w$ , chain number per aggregate  $N_{agg}$ , and density of the aggregates of PNiCD1-1 prepared at various heating rates. The  $N_{agg}$  was calculated by dividing  $M_w$  of aggregate by that of PNiCD1-1 ( $4.44 \times 10^5 \text{ g mol}^{-1}$ ). The density was obtained from  $4\pi\langle R_h \rangle^3/3M_w$

Heating rate/ $^\circ\text{C min}^{-1}$	$\langle R_h \rangle/\text{nm}$	PDI	$M_w/10^8 \text{ g mol}^{-1}$	$N_{agg}/10^3$	Density/ $\text{g cm}^{-3}$
0.033	136	0.034	8.0	2.0	0.12
0.2	112	0.058	4.1	0.93	0.12
0.33	101	0.073	2.9	0.66	0.11
0.5	62.1	0.051	2.2	0.50	0.36
1	53.0	0.092	1.7	0.39	0.45
30	42.7	0.074	0.72	0.16	0.37

Besides heating rate, the copolymer concentration in solution was found to affect the aggregation as well. As shown in Fig. 3b,  $\langle R_h \rangle$  of the final aggregates gradually increased as the copolymer concentration increased, when the same heating rate ( $0.2 \text{ }^\circ\text{C min}^{-1}$ ) was employed. This result was consistent with that found for other random copolymers containing PNIPAM and

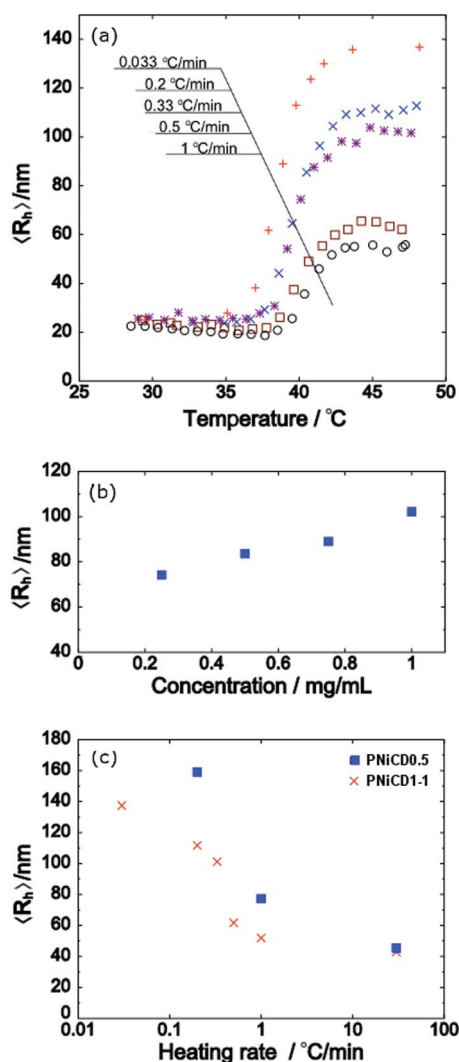


**Fig. 3** (a)  $\langle R_h \rangle$  plots of PNiCD1-1 during heating at various rates against temperature. (b)  $\langle R_h \rangle$  of the aggregates of PNiCD1-1 at different concentrations with a heating rate of  $0.2 \text{ }^\circ\text{C min}^{-1}$ . (c)  $\langle R_h \rangle$  of the aggregates of PNiCD1-1 and PNiCD0.5 at various heating rates.

hydrophilic moieties.<sup>25,44</sup> The influence of  $\beta$ -CD content in copolymer was also examined. The aggregates of PNiCD0.5 are much larger than that of PNiCD1-1 at the same heating rate (Fig. 3c). As the  $\beta$ -CD content in the former is about one half of that in the latter, it is understandable that less hydrophilic part,  $\beta$ -CD, which stabilizes the aggregate, would lead to larger micelles.

In order to explore the heating-rate dependence of the aggregation of copolymer PNiCD1-1, the size distributions of the final aggregates formed at different heating rate are compared. Fig. 4 shows both the unweighted (normal, intensity weighted)  $\langle R_h \rangle$  distributions (Fig. 4a) and 'mass-weighted'  $\langle R_h \rangle$  distributions (Fig. 4b) at  $48 \text{ }^\circ\text{C}$  obtained via different heating rate of PNiCD1-1. In principle, in the mass-weighted distribution, the contribution from small particles is more obvious than that in unweighted distributions. As shown in Fig. 4a of the unweighted plot, for all the different heating rates, monomodal distributions were observed although the peak position is different. However, in the mass-weighted plot in Fig. 4b, only for fast heating (curves of  $1 \text{ }^\circ\text{C min}^{-1}$ , and  $0.5 \text{ }^\circ\text{C min}^{-1}$ ), monomodal distributions, just as those in the unweighted plot, were obtained. For the cases with low heating rates ( $0.033, 0.2, 0.33 \text{ }^\circ\text{C min}^{-1}$ ), the copolymer aggregated into two types of species, as shown in peak A centered around  $10 \text{ nm}$ , and peak B with a larger  $\langle R_h \rangle$ , which is consistent with that shown in the unweighted curve. Considering the relatively small contribution to scattered light of the particles with smaller diameter, this result clearly demonstrates that in the slow heating process, the existence of the small particles associated to peak A cannot be neglected. The coexistence of both the large and small aggregates after slow heating process was confirmed by TEM and AFM (Fig. 5). In the TEM image of the sample obtained after slow heating process ( $0.033 \text{ }^\circ\text{C min}^{-1}$ ), not only particles with  $\langle R_h \rangle$  around  $136 \text{ nm}$  were clearly observed, a large population of small particles ( $\langle R_h \rangle = 10 \text{ nm}$ ) was found as well. This phenomenon was further confirmed by AFM, which also visualized these two different kinds of aggregated species of the same sample. However, for the sample obtained at a high heating rate ( $30 \text{ }^\circ\text{C min}^{-1}$ ), no particles with a small size around  $10 \text{ nm}$  were found, the particles are all the large ones.

The aggregation process of copolymer PNiCD1-1 was studied further by monitoring evolution of the distribution curves with increasing temperature at different heating rates. The unweighted and mass-weighted  $\langle R_h \rangle$  distribution curves obtained during slow ( $0.033 \text{ }^\circ\text{C min}^{-1}$ ) or fast ( $1.0 \text{ }^\circ\text{C min}^{-1}$ )

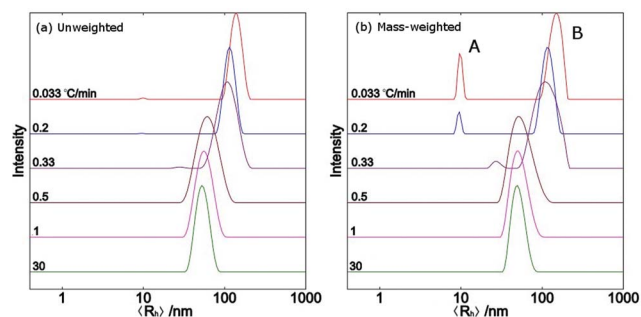


**Fig. 4** The left panel (a) shows the normalized unweighted size distributions and right panel (b) gives the mass-weighted data of the aggregates of PNiCD1-1 at  $48 \text{ }^\circ\text{C}$  for various heating rates.

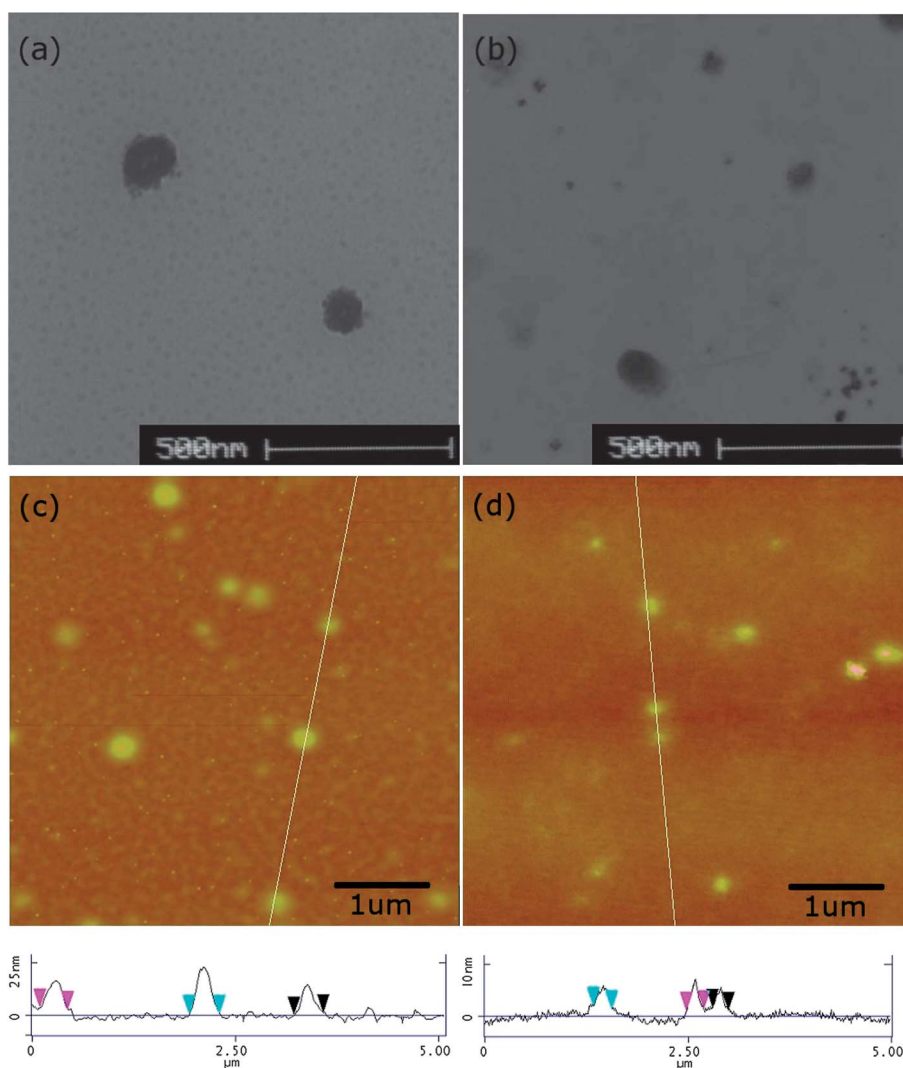


**Fig. 5** TEM and AFM images of PNiCD1-1 aggregates prepared at slow heating rate ( $0.2\text{ }^{\circ}\text{C min}^{-1}$ ) (a, c) and rapid heating rate ( $30\text{ }^{\circ}\text{C min}^{-1}$ ) (b, d), respectively. The height of cross sections along the white line in the AFM images is plotted at the bottom.

heating are shown in Fig. 6. In all the four plots of Fig. 6, at the beginning the samples showed a broad peak at  $25\text{ }^{\circ}\text{C}$ . Then the peak slightly shifted to smaller sizes indicating shrinking of individual chains due to the decrease of hydrophilicity of PNIPAM with temperature increase. Dramatic changes take place when the temperature reaches around  $38\text{ }^{\circ}\text{C}$ . In the unweighted plot for the slow heating process (Fig. 6a), the peak suddenly moves to a much higher size value and becomes much narrower at  $38\text{ }^{\circ}\text{C}$  and then shifts gradually to even a larger size with temperature increasing. However, in the mass-weighted plot Fig. 6b, when the temperature increases to around  $38\text{ }^{\circ}\text{C}$ , peak A became narrower and meanwhile a broad but small peak around  $100\text{ nm}$  (peak B) appears. Then the ratio of peak B vs. peak A continuously increases with temperature increasing, accompanying sharpening of peak B. At the end of the heating process at  $48\text{ }^{\circ}\text{C}$ , the intensity of peak B was much larger than that of peak A. Surprisingly, but consistent to the previous TEM and AFM results (Fig. 5a), peak A centring around  $10\text{ nm}$  remains. In addition, in the cooling process, the reverse change, *i.e.* the peak at  $110\text{ nm}$  directly immigrates into the peak at  $10\text{ nm}$ , was

observed (Fig. S4†). When a much faster heating process was employed, the difference between the unweighted and mass-weighted distributions was trivial. As shown in Fig. 6c and 6d, when the temperature surpasses the LCST, the original peak, becomes narrower with an obvious shift to some larger size. It is worth mentioning that, since the heating was really fast, at every temperature step, the duration was not long enough to correctly measure the quick-changing distributions in the transition region (Fig. 6). When temperature is beyond  $45\text{ }^{\circ}\text{C}$ , the curves almost do not change anymore with a peak located at  $53\text{ nm}$ . It is important to know that in the whole process of fast heating no stable small aggregates around  $10\text{ nm}$  were seen.

The heating rate dependence on the size of the aggregates actually is known from the previous reports for PNIPAM homopolymer and its random copolymers with hydrophilic units as well as graft copolymer with PEG branches.<sup>26</sup> Generally, the copolymer forms smaller aggregates in a fast heating process, while forms larger aggregates by slow heating. Obtaining the small aggregates was attributed to the domination of intramolecular aggregation in the fast heating process and further

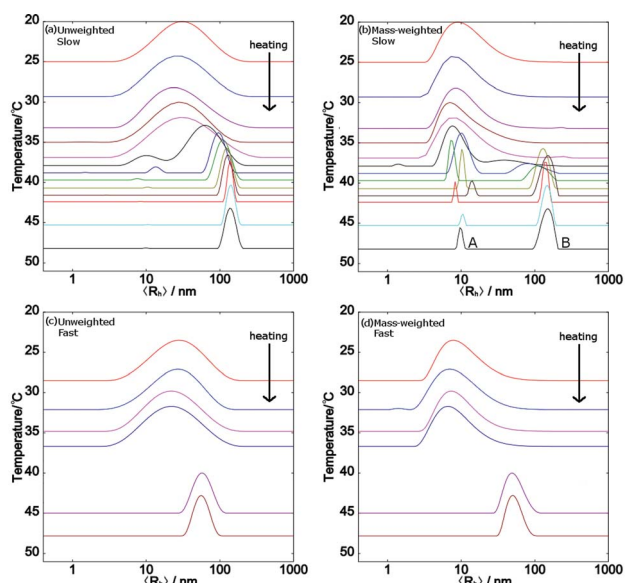


**Fig. 6** Size distributions by DLS during the heating process of the samples with slow stepwise heating ( $0.033\text{ }^{\circ}\text{C min}^{-1}$ ) for (a) and (b), and fast heating ( $1.0\text{ }^{\circ}\text{C min}^{-1}$ ) for (c) and (d), respectively. Unweighted results: (a) and (c) and mass-weighted results: (b) and (d).

growth of the aggregates was prevented due to the viscoelastic effect,<sup>45,46</sup> whereas the intermolecular and intramolecular aggregation competed in the slow heating process.

However, in the previous work,<sup>26</sup> no results on tracing the size distribution with time have been reported. So the coexistence of peak A and peak B found in the slow heating process in our experiment, which was not reported before, is hard to understand following the existing mechanism. Based on all the experimental results discussed above we would say that the key difference between the slow and fast heating processes is the exclusive existence of the stable small aggregates with a size around 10 nm in the slow heating process. Judging by the  $\langle R_h \rangle$  of 10 nm smaller than that of the parent copolymer chains, it is clear that the small aggregates are unimolecular micelles. In fact, the

unimolecular micelles with the hydrophobic part inside and the hydrophilic part outside were predicted in computational simulations for amphiphilic multi-block copolymers, graft copolymers, and random copolymers in dilute solution,<sup>9,28,47,48</sup> and they were also predicted as thermodynamically stable states in the scaling theory for the amphiphilic graft copolymer.<sup>48</sup> Besides, the unimolecular micelles were experimentally confirmed to be stable in the dilute solution for amphiphilic graft copolymer<sup>49,50</sup> and multi block copolymer.<sup>7</sup> Considering that PNiCD is a random copolymer with bulky hydrophilic CD side groups, formation of unimolecular micelles is expectable. However, formation of such unimolecular micelles from dissolved polymer chains requires complicated conformation adjustments. For our copolymer, which is relatively rigid in water, such conformation alternation is more difficult than that for ordinary flexible copolymers. In the slow heating process, increasing the temperature at the earlier stage from room temperature to around  $38\text{ }^{\circ}\text{C}$  took about 30–300 min during which sharpening of peak A occurred indicating the formation of the unimolecular micelles. It was followed by a drastic turning of the PNiCD main chain to hydrophobicity, so peak B appeared and finally reached its stable and narrow state around  $43\text{ }^{\circ}\text{C}$ . The growth of peak B was at the expenses of peak A. So we have reasons to think that the larger aggregates were formed as a result of the secondary aggregation of the small unimolecular micelles in order to cope with the increasing hydrophobicity of the PNiCD main chains (Fig. 7). In contrast, in the fast heating process *e.g.*  $1\text{ }^{\circ}\text{C min}^{-1}$ , increasing the temperature from room temperature to around  $38\text{ }^{\circ}\text{C}$  only takes about 10 min, in such a short duration, only local chain shrinkage and collapse is possible, so no unimolecular micelles form. Then the temperature rapidly increases to above  $38\text{ }^{\circ}\text{C}$ , where the PNiCD main chain drastically loses its hydrophilicity, which thus causes both intramolecular and intermolecular aggregation (Fig. 7). These resultant aggregates would not be able to grow into even larger particles because the temperature becomes much higher than the LCST very quickly, so dehydration of the PNiCD chains becomes completed and the chains are ‘frozen’, unable to stick to each other further. Thus the resultant

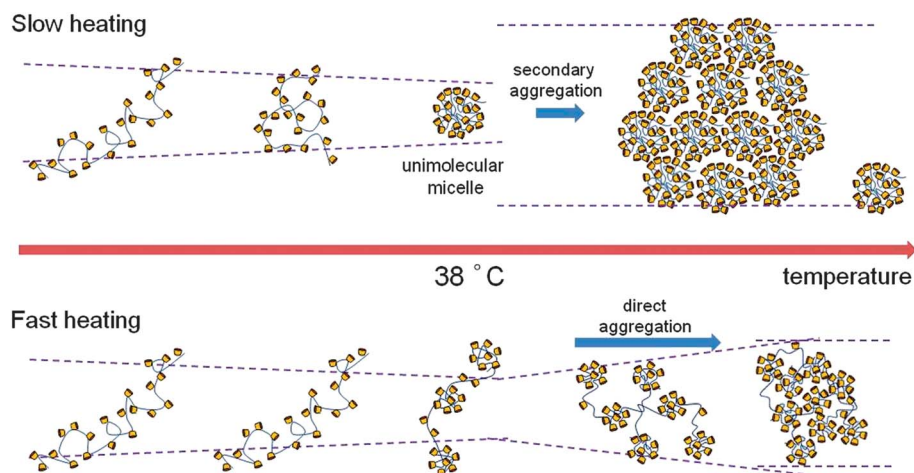


**Fig. 7** The scheme of two different aggregation mechanisms for slow heating and fast heating processes. In the slow heating process, the PNiCD copolymer chain gradually reorients into intramolecular micelle during early period in the transition, and then the micelles aggregate again into secondary micelles with further temperature elevation. In contrast, the PNiCD chain in the fast heating process cannot form intramolecular micelles and directly entangles and fuses with other chains, resulting in the formation of randomly packed aggregation.

aggregates are much smaller than those from the slow heating process. A schematic illustration of the two mechanisms in the fast and slow heating is shown in Fig. 7.

The two mechanisms suggested above are also supported by the density data of the final aggregates, which are calculated from  $\langle R_h \rangle$  and  $M_w$ , as summarized in Table 4. The density of the aggregates prepared after slow heating (0.033, 0.2, 0.33 °C min<sup>-1</sup>) is about 0.12 g cm<sup>-3</sup>, which is obviously smaller than that prepared by fast heating (0.5, 1.0, and 30 °C min<sup>-1</sup>), i.e. 0.36–0.45 g cm<sup>-3</sup>. It is clear that the low density for the case of slow heating reflects the loose packing of the secondary aggregation of the unimolecular micelles while the high density for the fast heating represents the relatively compact random aggregation.

## Conclusions

A series of random copolymers of poly[(*N*-isopropyl acrylamide)-*co*-(aminoethyl methacrylate  $\beta$ -cyclodextrin)] (PNiCD) were prepared and investigated. SLS and DLS studies show that the copolymer has a rather rigid conformation, which can be attributed to the presence of the pendent bulky CD groups along the copolymer main chain. The copolymer PNiCD is easily grafted by other polymer chains with a guest moiety on the chain end. The grafting density depends on the binding ability of the guests to CDs. When the neat copolymer is heated above its LCST, thermo-induced self-assembly takes place, leading to aggregates, the size of which depends on the heating rates. In slow heating, the copolymer forms unimolecular micelles with  $\langle R_h \rangle$  10 nm first and then the micelles combine to form loose and large aggregates, around 100–140 nm. However, in fast heating, direct random aggregation occurs, leading to compact aggregates with  $\langle R_h \rangle$  about 40–60 nm. The difference in the two mechanisms is caused by the fact that the formation of the unimolecular micelles needs difficult conformation adjustment of the copolymer chains, which can only be performed if the heating rate is slow enough.

## Acknowledgements

National Natural Science Foundation China (No. 20834004 and No. 20904005) and Ministry of Science and Technology of China (2009CB930402 and 2011CB932503) are acknowledged for financial support.

## Notes and references

- 1 N. Nishiyama and K. Kataoka, *Pharmacol. Ther.*, 2006, **112**, 630–648.
- 2 R. K. O'Reilly, C. J. Hawker and K. L. Wooley, *Chem. Soc. Rev.*, 2006, **35**, 1068–1083.
- 3 P. Tanner, P. Baumann, R. Enea, O. Onaca, C. Palivan and W. Meier, *Acc. Chem. Res.*, 2011, **44**, 1039–1049.
- 4 Y. Wan, Y. Shi and D. Zhao, *Chem. Mater.*, 2007, **20**, 932–945.
- 5 B. Fang, A. Walther, A. Wolf, Y. Xu, J. Yuan and A. H. E. Müller, *Angew. Chem., Int. Ed.*, 2009, **48**, 2877–2880.
- 6 G. Sun, H. Cui, L. Y. Lin, N. S. Lee, C. Yang, W. L. Neumann, J. N. Freskos, J. J. Shieh, R. B. Dorshow and K. L. Wooley, *J. Am. Chem. Soc.*, 2011, **133**, 8534–8543.
- 7 Y. Zhou, K. Jiang, Q. Song and S. Liu, *Langmuir*, 2007, **23**, 13076–13084.
- 8 I. R. Cooke and D. R. M. Williams, *Macromolecules*, 2003, **36**, 2149–2157.
- 9 V. Hugouvieux, M. A. V. Axelos and M. Kolb, *Macromolecules*, 2009, **42**, 392–400.
- 10 E. A. Appel, F. Biedermann, U. Rauwald, S. T. Jones, J. M. Zayed and O. A. Scherman, *J. Am. Chem. Soc.*, 2010, **132**, 14251–14260.

- 11 J. Geng, F. Biedermann, J. M. Zayed, F. Tian and O. A. Scherman, *Macromolecules*, 2011, **44**, 4276–4281.
- 12 J. Geng, D. Jiao, U. Rauwald and O. A. Scherman, *Aust. J. Chem.*, 2010, **63**, 627–630.
- 13 A. R. Hajipour, S. Habibi and A. E. Ruoho, *J. Appl. Polym. Sci.*, 2010, **118**, 818–826.
- 14 T. Ogoshi, K. Masuda, T. Yamagishi and Y. Nakamoto, *Macromolecules*, 2009, **42**, 8003–8005.
- 15 B. M. Rambo, S. K. Kim, J. S. Kim, C. W. Bielawski and J. L. Sessler, *Chem. Sci.*, 2010, **1**, 716–722.
- 16 F. Vocanson, P. Seigle-Ferrand, R. Lamartine, A. Fort, A. W. Coleman, P. Shahgaldian, J. Mugnier and A. Zerroukhi, *J. Mater. Chem.*, 2003, **13**, 1596–1602.
- 17 (a) S. Ren, D. Chen and M. Jiang, *J. Polym. Sci., Part A: Polym. Chem.*, 2009, **47**, 4267–4278; (b) S. Ren, D. Chen and M. Jiang, *Gaodeng Xuexiao Huaxue Xuebao*, 2010, **31**, 167–171.
- 18 S. Tamesue, Y. Takashima, H. Yamaguchi, S. Shinkai and A. Harada, *Angew. Chem., Int. Ed.*, 2010, **49**, 7461–7464.
- 19 J. Zhang, H. Sun and P. X. Ma, *ACS Nano*, 2010, **4**, 1049–1059.
- 20 A. Bertrand, S. Chen, G. o. Souharce, C. Ladavière, E. Fleury and J. Bernard, *Macromolecules*, 2011, **44**, 3694–3704.
- 21 (a) P. Guo, W. Guan, L. Liang and P. Yao, *J. Colloid Interface Sci.*, 2008, **323**, 229–234; (b) X. Liu, J. Kim, J. Yu and A. Eisenberg, *Macromolecules*, 2005, **38**, 6749–6751; (c) Y. Li, Y. Deng, X. Tong and X. Wang, *Macromolecules*, 2006, **39**, 1108–1115.
- 22 (a) X. Liu, C. Yi, Y. Zhu, Y. Yang, J. Jiang, Z. Cui and M. Jiang, *J. Colloid Interface Sci.*, 2010, **351**, 315–322; (b) X. Liu, Y. Wang, C. Yi, Y. Feng, J. Jiang, Z. Cui and M. Chen, *Chin. J. Chem.*, 2009, **67**, 447–452.
- 23 J. Xu, Z. Zhu, S. Luo, C. Wu and S. Liu, *Phys. Rev. Lett.*, 2006, **96**, 027802.
- 24 X. Ye, Y. Lu, L. Shen, Y. Ding, S. Liu, G. Zhang and C. Wu, *Macromolecules*, 2007, **40**, 4750–4752.
- 25 H. Chen, J. Li, Y. Ding, G. Zhang, Q. Zhang and C. Wu, *Macromolecules*, 2005, **38**, 4403–4408.
- 26 H. Chen, Q. Zhang, J. Li, Y. Ding, G. Zhang and C. Wu, *Macromolecules*, 2005, **38**, 8045–8050.
- 27 A. Byrne, P. Kiernan, D. Green and K. A. Dawson, *J. Chem. Phys.*, 1995, **102**, 573.
- 28 Y. A. Kuznetsov, E. G. Timoshenko and K. A. Dawson, *J. Chem. Phys.*, 1995, **103**, 4807.
- 29 Y. A. Kuznetsov, E. G. Timoshenko and K. A. Dawson, *J. Chem. Phys.*, 1996, **104**, 3338.
- 30 K. A. Connors, *Chem. Rev.*, 1997, **97**, 1325–1358.
- 31 E. M. M. Del Valle, *Process Biochem.*, 2004, **39**, 1033–1046.
- 32 M. V. Rekharsky and Y. Inoue, *Chem. Rev.*, 1998, **98**, 1875–1918.
- 33 H. Schneider, *Angew. Chem., Int. Ed. Engl.*, 1991, **30**, 1417–1436.
- 34 (a) J. Wang and M. Jiang, *J. Am. Chem. Soc.*, 2006, **128**, 3703–3708; (b) J. Wang and M. Jiang, *Gaofenzi Xuebao*, 2007, **10**, 979–985.
- 35 J. Zhang and P. X. Ma, *Nano Today*, **5**, pp. 337–350.
- 36 J. Zeng, K. Shi, Y. Zhang, X. Sun and B. Zhang, *Chem. Commun.*, 2008, 3753.
- 37 M. Nakahata, Y. Takashima, H. Yamaguchi and A. Harada, *Nat. Commun.*, 2011, **2**, 511.
- 38 H. Ohashi, Y. Hiraoka and T. Yamaguchi, *Macromolecules*, 2006, **39**, 2614–2620.
- 39 A. Bertrand, M. Stenzel, E. Fleury and J. Bernard, *Polym. Chem.*, 2012, **3**, 377–383.
- 40 J. Stadermann, H. Komber, M. Erber, F. Dáritz, H. Ritter and B. Voit, *Macromolecules*, 2011, **44**, 3250–3259.
- 41 A. O. Moughton and R. K. O'Reilly, *J. Am. Chem. Soc.*, 2008, **130**, 8714–8725.
- 42 C. Wang, Q. Chen, H. Xu, Z. Wang and X. Zhang, *Adv. Mater.*, 2010, **22**, 2553–2555.
- 43 J. Zou, B. Guan, X. Liao, M. Jiang and F. Tao, *Macromolecules*, 2009, **42**, 7465–7473.
- 44 J. Yan, W. Ji, E. Chen, Z. Li and D. Liang, *Chin. J. Polym. Sci.*, 2010, **28**, 437.
- 45 H. Tanaka, *Macromolecules*, 1992, **25**, 6377–6380.
- 46 H. Tanaka, *Phys. Rev. Lett.*, 1993, **71**, 3158–3161.
- 47 O. V. Borisov and E. B. Zhulina, *Macromolecules*, 2005, **38**, 2506–2514.
- 48 P. Kosövan, J. Kuldová, Z. Limpouchová, K. Procházka, E. B. Zhulina and O. V. Borisov, *Macromolecules*, 2009, **42**, 6748–6760.
- 49 A. Kikuchi and T. Nose, *Polymer*, 1996, **37**, 5889–5896.
- 50 C. Wu and X. Wang, *Phys. Rev. Lett.*, 1998, **80**, 4092.